An Atom-Probe Study of Retained Austenite in Ferritic Weld Metal

High-resolution analytic techniques are used to quantitatively prove the distribution of boron and carbon in weld metal

BY M. N. CHANDRASEKHARAIAH, G. DUBBEN AND B. H. KOLSTER

ABSTRACT. The addition of titanium and boron to welding consumables results in an acicular ferrite microstructure that imparts excellent toughness to the weldment. An atom-probe field-ion microscopic study was carried out to study the influence of carbon and boron on the γ–α transformation in a ferritic weld metal and on the formation of acicular ferrite. It was observed that carbon diffuses into the remaining austenite when acicular ferrite is formed. The retained austenite can be enriched up to 7 at.-% with carbon, and it showed to be stable at a temperature of 90 K after removing some of the surrounding acicular ferrite grains. The atom-probe analysis did not indicate the presence of boron either at the γ–α interface or in the retained austenite grain.

Introduction

The addition of titanium and boron in small amounts to welding consumables is known to improve the toughness of the resulting ferritic weld metals (Refs. 1, 2). According to the literature, titanium reduces the formation of boron oxides and nitrides so that a sufficient amount of free boron is available. These free boron atoms can diffuse to austenite grain boundaries resulting in a retardation of the γ–α transformation at these boundaries. The resulting microstructure within the grains consists primarily of acicular ferrite and a mixture of very small amounts of pearlite, bainite, martensite and retained austenite.

Several workers have studied the formation of acicular ferrite in welds (Refs. 3, 4). From electron microscopic studies on partially and fully transformed weld microstructures, it has been proposed that acicular ferrite nucleates at intragranular inclusion sites present in the prior austenite grains. During the γ–α transformation, the carbon supersaturation in the ferrite can be relieved by either precipitation of carbides within the ferrite, or by partitioning of carbon in the remaining austenite by means of diffusion. This residual austenite either may transform into a large variety of microstructural constituents such as pearlite, upper and lower bainite and martensite, or it can remain as intragranular islands within the acicular ferrite structure.

It is clear that the (re)distribution of elements like boron and carbon among the various constituents is an important factor in the course of the acicular ferrite transformation. The transmission electron microscope has been used by many investigators to study the crystallography and morphology of fine-scale precipitates, but the resolution has been found to be inadequate to study the effect of boron and carbon on an atomic scale. In the present work, an atom-probe field-ion microscope was used to provide direct quantitative proof for the distribution of boron and carbon on an ultra-high resolution scale. The results presented here are a part of a larger program investigating the effect of titanium and boron on weld metal structures (Ref. 5). Detailed electron microscopic and atom-probe field-ion microscopic study of the weldments are reported elsewhere (Refs. 2, 5, 6). Several interfaces have been examined, and the present results represent a typical case study to highlight the high-resolution capability of the analytical techniques used and their significance and application in the microstructural study of weldments.

KEY WORDS

Ferritic Weld Metal
Atom-Probe Study
Retained Austenite
Acicular Ferrite
Field Ion Microscopy
Gamma-Alpha Transformation
Ti and B Effects
Flux Cored Arc Welds
Mass Sprectrum
Stabilized Austenite

Experimental Procedures

The test specimens used in this investigation are from a multipass flux cored arc weld. The welding was carried out using a flux cored wire with trace amounts of titanium and boron on a 20-mm (0.8-in.) thick St-EH 36 steel plate. The weld was manufactured using an electrode with trace amounts of titanium and boron. The welding conditions were 320 A (DC electrode positive), 30.5 V for all eight passes with a heat input of 19–20 kJ/cm (48–51 kJ/in.). The weld metal composition is given in Table 1.

Small sections of size 25 X 5 X 5 mm (1 X 0.2 X 0.2 in.) were cut from the top layer in such a way that the long side was parallel to the weld direction. Care was taken by macroetching the weld cross-section so that the cut section lies

M. N. CHANDRASEKHARAIAH is with Welding Research Institute, BHEL, Tiruchirapalli, India. G. DUBBEN is with Ned. Philips Bedrijven B.V. Eindhoven, The Netherlands. B. H. KOLSTER is with Materials Science Section, Department of Mechanical Engineering, University of Twente, Enschede, The Netherlands.

Table 1 — Chemical Composition of the Weld Metal

	C	Mn	Si	P	S	Ti	B	N	O	Fe
wt-%	0.087	1.37	0.62	0.017	0.009	0.051	0.0085	0.009	0.050	bal

in the weld pool. The sections were reduced to needles of 0.5 X 0.5 mm (0.02 X 0.02 in.) cross-sections by electrodischarge machining. Subsequently, these sections were thinned to a diameter of about 0.4 mm (0.016 in.) by electropolishing in an electrolyte containing 6% perchloric acid in 94% acetic acid. The final tip shape was achieved by using a special electropolishing setup, in which a gold wire loop holds a film of 3% perchloric acid in butyloxy ethanol. The polished specimens were first examined in the transmission electron microscope for the tip profile as well as for the presence of grain boundaries and small precipitates, which are amenable for examination in the atom-probe field-ion microscope. Even though the volume of specimen examined in the atom-probe field-ion microscope is very small ($\sim 10^{-15}$ cm^3) the use of transmission electron microscopy, in conjunction with the atom-probe, ensures that each of the needles examined has the desired features such as boundaries and precipitates.

The field-ion microscope/atom probe used in this study consists of a straight time of flight mass spectrometer (Ref. 7). The imaging of the specimen was carried out by using neon gas (pressure 1.3 X 10^{-3} Pa). For each mass spectrum, a total of 1000 ions was collected, using a pulse fraction (V_p/V_{dc}) of 20% and a background pressure of the neon gas of 1.3 X 10^{-5}Pa. The ion collection rate was 1 ion per 10 to 20 pulses with a pulse repetition rate of 40 Hz.

Results

Figure 1 shows the microstructure of the top layer of the weld, where acicular ferrite is the dominant constituent.

The shape of the field-ion specimen is shown in the dark field electron micrograph (Fig. 2). From what follows, it can be concluded that in this micrograph retained austenite appears as the dark-imaged phase and the acicular ferrite as the bright one.

In the field-ion microscope/atom probe, the image of retained austenite started to appear at 5.8 kV. After sufficient field evaporation, the austenite-ferrite interface could be observed at 11.7 kV — Fig. 3A. The first indication for the presence of retained austenite in the field-ion image (Fig. 3A) is the darkness of the image with the appearance of several bright spots, which has been found for steels (Refs. 8, 9) and weld metal (Ref. 10). It was impossible to determine the orientation of this phase due to lack of presence of adequate poles in the field-ion microscopic images. The ferritic phase gives the usual bright image, which grows with the removal of an increasing amount of atomic layers (Fig. 3B and C). Finally, after further continued field evaporation, the interface disappeared, leaving merely ferrite. In the ferrite, the poles could be observed clearly (Fig. 3D).

A mass spectrum of retained austenite is shown in Fig. 4A. This corresponds to the probe hole position in the field-ion micrograph in Fig. 3A. Carbon peaks were observed at mass-to-charge ratios (m/n) of 6, 12, 18 and 24, which corresponds to C^{2+}, C^{+}, C^{2+}_3 and C^{+}_2. So, not only monomers of carbon exist, but also polycarbon ions are present. Out of the total carbon present in the retained austenite nearly half is in the polycarbon form. In Fig. 4B (corresponding to the probe hole position in Fig. 3D) a mass spectrum of ferrite is shown in which the different isotopes of silicon and iron can be observed at m/n ratios of 14, 14.5 and 15 for silicon, and m/n ratios for iron at 27, 28, 28.5 and 29. These ratios correspond to 28 Si^{2+}, 29 Si^{2+}, 30 Si^{2+}, 54 Fe^{2+}, 56 Fe^{2+}, 57 Fe^{2+} and 58 Fe^{2+}.

The composition profile determined across the retained austenite, the ferrite and their interface is shown in Fig. 5. The extent of the interface region is partly due to the transition region of the grain boundary, partly to the probe hole size and the oblique crossing of the phase boundary through the tip. The carbon concentration reaches a peak value of 6.8 at.-% near the interface of the retained austenite and shows a concentration of 2 at.-% in the interior. This high carbon concentration is the second indication that the phase under consideration is retained austenite. It should be noticed that near the interface in the ferrite the carbon concentration drops drastically to zero. In the case of Mn and Si,

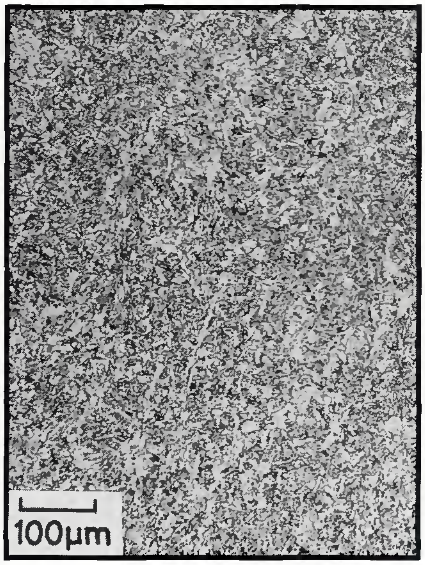

Fig. 1 — Microstructure of the weld metal.

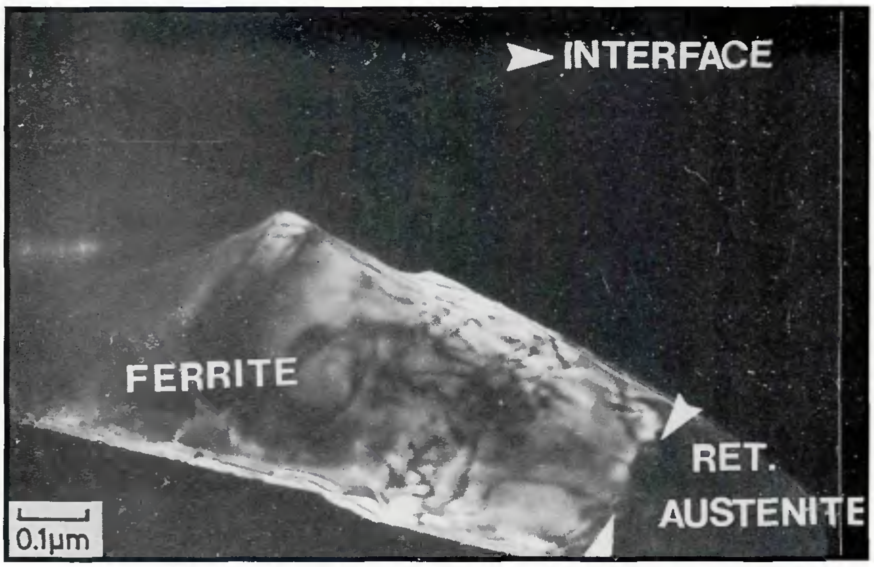

Fig. 2 — Dark field electron micrograph of the field-ion specimen.

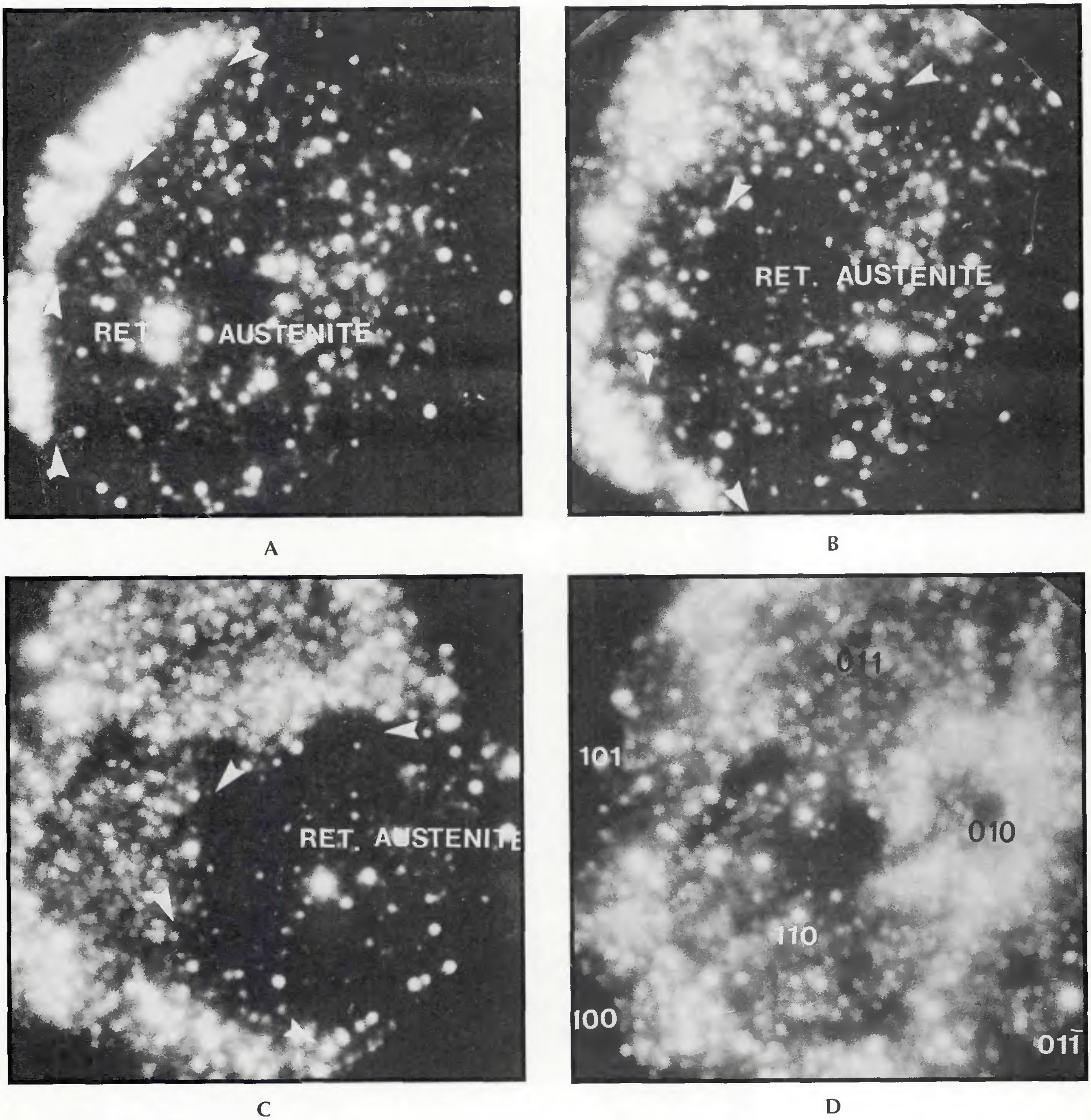

Fig. 3 — Field-ion images after different stages of field evaporation, showing the retained austenite-ferrite interface as a function of field evaporation. A — Taken at 11.7 kV; B — 13.2 kV; C — 13.6 kV; D — 15.5 kV.

no significant difference in concentration is found. Finally, it should be stressed that no boron was found in this sample, neither in the phases nor in the interface region.

Discussion

The retained austenite is identified in the field-ion microscope/atom probe by the dark-field images and from its composition. The atom probe results show that carbon diffusion from the transformed region to the remaining austenite has taken place during the γ-α transformation. This results in carbon-enriched austenite, which remains stable down to the tip temperature of 90 K. Investigations on retained austenite in steels (Refs. 8, 9) and weld metal (Ref. 10) indicated similar results.

It is remarkable to see that retained austenite was stable during observation in the field-ion microscope/atom probe. There can be several explanations why retained austenite is stable, namely:

1) Retained austenite could be chemically stabilized through carbon. For the weld metal used, the M_s temperature is 475°C (887°F) (Ref. 13). Because of the carbon concentration of about 2 at.-%, the M_s temperature will be lowered by about 100°C (180°F) (Ref. 8). Since at

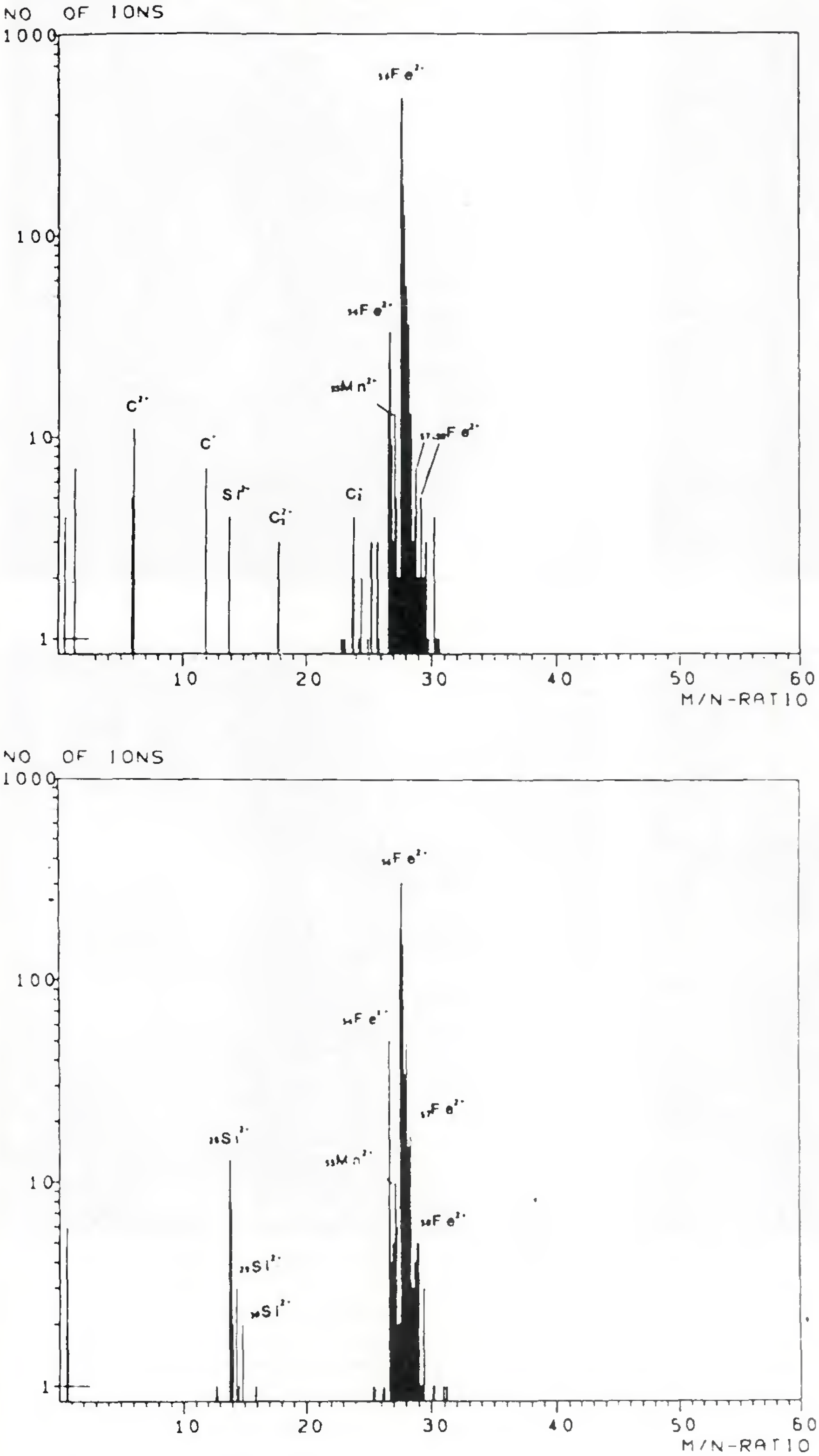

Fig. 4 — A — Mass spectrum of retained austenite; B — mass spectrum of ferrite.

this concentration the M_f temperature is about 200°C (360°F) lower than M_s, it can be concluded that the M_f temperature of this phase will be around 175°C (347°F). So, it may be expected that the austenite cannot be retained down to room temperature because of the carbon enrichment.

2) It is known that retained austenite is stabilized because of the pressure exerted by the surrounding matrix. The austenite in the field-ion microscope specimen, however, is free from any such constituents. So, transformation of the austenite into martensite should occur.

3) For dual phase steels (Ref. 11), it is known that the particle size can be a stabilizing factor. It has been observed that particles with a size less than 1µm do not transform, while larger ones do. The reason for this particle size effect is not clearly understood. It has been suggested that the particle size of 1µm or less may be too small to contain a martensite nucleus (Ref. 12). From transmission electron microscopy and field-ion microscopy/atom probe, the particle size could be determined to be about 0.15 µm, which is indeed smaller than 1 µm.

It is interesting to note that no boron was found in the interface region. Other investigations (Ref. 2) have shown that a considerable amount of boron can be present at the γ-α interface. From transformation studies (Ref. 13) it is known that the γ-α transformation starts around 615°C. Besides, it is known that boron is present in the ferrite grains (Ref. 6). Taking all this into consideration, there is a tentative explanation why boron is not located at the interface under consideration. This is because the diffusion of boron is not sufficient at temperatures below 615°C and at the cooling rates applied. Only in the case where the retained austenite is formed at the original γ-α interface, when enough boron is accumulated during cooling in this γ region, boron will be found at the γ-α interface (Ref. 2).

The results obtained by van Scherpenzeel, *et al.* (Ref. 13), refers to this situation, and additional work is needed to substantiate this hypothesis.

Conclusions

The following conclusions can be drawn from the field-ion microscope/atom probe investigations of the retained austenite and its interface in titanium- and boron-containing weld metal:

1) The retained austenite is surrounded by acicular ferrite.

2) During the acicular ferrite formation from austenite, the remaining

austenite is enriched with carbon, up to about 7 at.-% .and it drops down to about 2 at. % at the γ-α interface.

3) Retained austenite was stable at 90 K, and the only conceivable explanation for this observation is the smaller grain size of 0.1 to 0.2 μm.

4) Boron was not present at the γ-α-interface, which means that diffusion of boron to this type of interface did not occur below 615°C.

Acknowledgment

The authors would like to thank Filarc Welding Industries (earlier Philips Welding Industries) for preparing the weld material and for its continuing interest in the work.

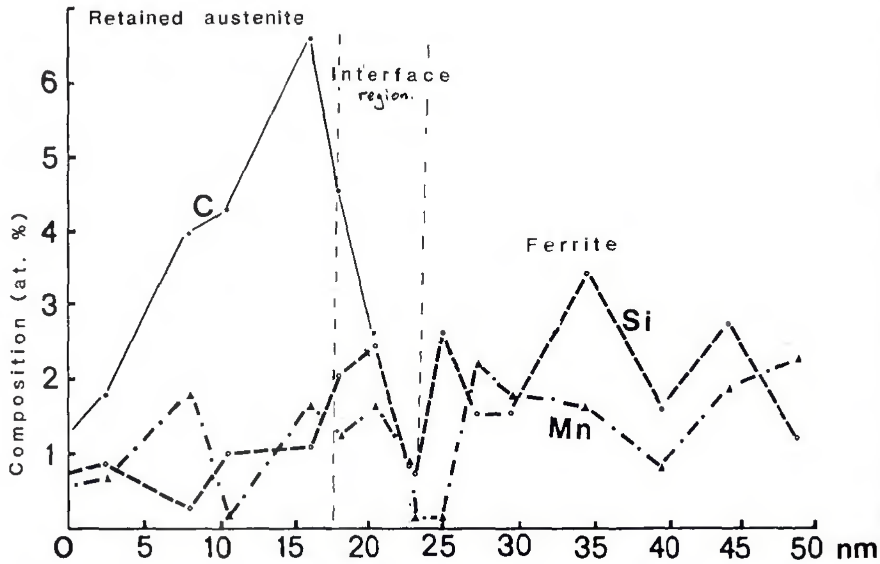

Fig. 5 — Composite profile of the different elements across the retained austenite-ferrite interface.

References

1. Devletian, J. H., and Heine, R. W. 1975. *Welding Journal* 54(2).

2. Tiersma, V., Dubben, G., Mandziej, S., Goldschmitz, M. A., and Kolster, B. H. 1987. Proc. Intern. Welding Conf., New Delhi, India.

3. Ricks, R. A., Howell, P. R., and Barritte, G. S. 1982. J.Mat. Sci., 17, p. 732.

4. Mori, N., *et al.* 1981. IIW Doc. 1196-81.

5. Dubben, G., Chandrasekharaiah, M. N., Beyer, J., and Kolster, B. H. 1985. *Journal de Physique*, 46, C9.

6. Dubben, G., Chandrasekharaiah, M. N., and Kolster, B. H. J.Mat.Sci. (in press).

7. Bach, P. W. 1981. Ph.D. thesis, University of Twente, The Netherlands.

8. Brenner, S. S., Miller, M. K., and Fisher, R. M. 1981. 28th Intern. Field Emission Symp. Portland, Ore.

9. Barnard, S. J., Smith, G. D. W., Miller, M. K., Brenner, S. S., Sarikaya, M., and Thomas, G. 1981. 28th Intern. Field Emission Symp. Portland, Ore.

10. Beyer, J., and Bach, P. W. 1981. 28th Intern. Field Emission Symp. Portland, Ore.

11. Lanzilloto, C. A. N., and Pickering, F. B. 1982. Met. Sci., L6, p. 371.

12. Ballinger, N. K., and Cladman, T. 1982. Met. Sci., 15, p. 95.

13. Scherpenzeel, E. van, *et al.*, to be published.

WRC Bulletin 363
May 1991

Recommended Practices in Elevated-Temperature Design: A Compendium of Breeder Reactor Experiences (1970–1987), Volume II—Preliminary Design and Simplified Methods

Edited by A. K. Dhalla

The recommended practices for elevated-temperature design of liquid metal fast breeder reactors (LMFBR) have been consolidated into four volumes to be published in four individual WRC bulletins.

Volume I: Current Status and Future Directions (WRC Bulletin 362)
Volume II: Preliminary Design and Simplified Methods (WRC Bulletin (363)
Volume III: Inelastic Analysis (WRC Bulletin 365)
Volume IV: Special Topics (WRC Bulletin 366)

In Volume II, preliminary design procedures are described that provided practical design and analysis guidelines for specific structural design problems encountered in the past. Also included is a detailed discussion of simplified methods to support both preliminary and final design evaluations.

Publication of this bulletin was sponsored by the Committee on Elevated Temperature Design of the Pressure Vessel Research Council. The price of WRC Bulletin 363 is $40.00 per copy, plus $5.00 for U.S. and $10.00 for overseas, postage and handling. Orders should be sent with payment to the Welding Research Council, Room 1301, 345 E. 47th St., New York, NY 10017.

WRC Bulletin 368
November 1991

Stresses in Intersecting Cylinders Subjected to Pressure

By K. Mokhtarian and J. S. Endicott

This bulletin has been prepared to provide the designer with a simple and approximate method of calculating maximum stresses due to internal pressure at cylinder intersections. Formulas are provided for calculating membrane and bending stresses in both the vessel and the nozzle. However, this bulletin does not present any rules for design, but it is rather intended to be an aid in assessing the local structural integrity of the vessel.

Publication of this report was sponsored by the Committee on Reinforced Openings and External Loadings of the Pressure Vessel Research Council. The price of WRC Bulletin 368 is $30.00 per copy, plus $5.00 for U.S. and $10.00 for overseas, postage and handling. Orders should be sent with payment to the Welding Research Council, Room 1301, 345 E. 47th St., New York, NY 10017.